Journal of Power Sources 189 (2009) 607–610

Contents lists available at ScienceDirect

Journal of Power Sources

journal homepage: www.elsevier.com/locate/jpowsour

Short communication

Enhanced capacity retention of Co and Li doubly doped $LiMn_2O_4$

Changyin Wang, Shigang Lu*, Surong Kan, Jing Pang, Weiren Jin, Xiangjun Zhang

Energy Materials and Technology Research Institute, General Research Institute for Nonferrous Metals, Beijing 100088, PR China

ARTICLE INFO

Article history:
Received 28 June 2008
Received in revised form 28 August 2008
Accepted 20 September 2008
Available online 7 October 2008

Keywords:
Doped $LiMn_2O_4$
Cycling performance
Mn dissolution
Structural stability
Lithium-ion batteries

ABSTRACT

Cobalt and lithium doubly doped spinel $LiMn_2O_4$ have been synthesized by a solid state reaction. The effect of Co and Li doped spinel $LiMn_2O_4$ was investigated. The undoped and doped spinels were characterised by means of X-ray diffraction (XRD), inductively coupled plasma/atomic emission spectrometer (ICP/AES) and electrochemical test. The results showed that the doped spinel exhibited superior cycling performance than undoped spinel. The capacity retention of graphite/doped spinel full cell was more than 86% after 1000 cycles (2*C* rate) at room temperature, which maintained 85% after 100 cycles (1*C* rate) at 55 °C. The differential capacity profiles on doped spinel cathode are more fixed than undoped spinel cathode. Compared with undoped spinel, Mn dissolution into electrolyte at 55 °C was reduced by 41%, the lattice parameter difference Δa was reduced by 82% on doped spinel cathode after cycling. The greatly suppressed structural change and manganese dissolution are responsible for the improved cycling performance on cobalt and lithium doubly doped spinel.

1. Introduction

Spinel $LiMn_2O_4$ is considered as the most promising cathode material for lithium-ion batteries due to its advantages such as low cost, abundant in nature, environment benign [1–5]. However, $LiMn_2O_4$ cathode has severe capacity fading during cycling, especially at elevated temperature [1–10]. This problem has been hindering its application all along. Researchers have made extensive work to enhance cycling performance. The capacity fading mechanisms on spinel $LiMn_2O_4$ are complex and not fully understood [3], several reasons are considered to explain its poor cycling performance, including structural instability, Jahn–Teller distortion and Mn dissolution into electrolyte [5–10], etc. It has been reported that Mn ions substituted by other elements can suppress structural change and manganese dissolution [10–20].

In this paper, we investigated the effect of Co and Li doubly doped spinel $LiMn_2O_4$, the reason for improved cycling performance was discussed.

2. Experimental

Doped spinel $LiMn_2O_4$ was synthesized by mixing stoichiometric amounts of $LiCoO_2$, Li_2CO_3, and bare $LiMn_2O_4$ (Qingdao Qianyun Co., Ltd.) (mole ratio 0.1:0.025:1), the mixture was calcined at 730 °C for several hours to obtain doped $LiMn_2O_4$, the composition of the doped $LiMn_2O_4$ is $Li_{1.05}Co_{0.10}Mn_{1.85}O_4$.

The structure of undoped $LiMn_2O_4$, doped $LiMn_2O_4$ and their cycled electrodes were characterised by X-ray diffraction (XRD). The specific surface area was measured by Brunauer–Emmett–Teller method (BET). The manganese dissolution was assessed by soaking 0.5 g spinel samples in 5 ml electrolyte solution at 55 °C for 7 days and determining the amount of Mn into the electrolyte by inductively coupled plasma/atomic emission spectrometer (ICP/AES).

The electrochemical performance of spinel samples was evaluated using half cell (Li/spinel) and full cell (graphite/spinel).

In the half cell, cathodes were prepared by coating the slurry of 88 wt.% spinel, 6 wt.% graphite, 2 wt.% acetylene black (AB) and 4 wt.% polyvinylidene fluoride (PVDF) dissolved in *N*,*N* dimethylforamide (DMF) on aluminium foil. Lithium metal was used as anode.

In the full cell, cathodes were prepared by coating the slurry of 87 wt.% spinel, 3 wt.% KS-6 (Timcal Co., Ltd.), 5 wt.% carbon black and 5 wt.% PVDF dissolved in *N*-methylpyrrolidone (NMP) on aluminium foil. The anodes were prepared by coating the slurry of 83 wt.% compound artificial graphite (CMP-2, Shanshan Tech Co., Ltd.), 10 wt.% KS-6 and 7 wt.% PVDF dissolved in *N*-methylpyrrolidone on copper foil. The electrolyte was 1 M $LiPF_6$–ethylene carbonate/diethyl carbonate (EC/DEC, 1:1, v/v). The capacity ratio of positive and negative electrodes of the "full cell" is 100/110. The capacities of the anodes are large enough to avoid influences on the cycle life. The shape of the full cell is prismatic, the model is 053450, the cell has external dimensions of thickness

* Corresponding author. Tel.: +86 10 82241928; fax: +86 10 62055412.
E-mail address: slu@grinm.com (S. Lu).

0378-7753/$ – see front matter © 2008 Elsevier B.V. All rights reserved.
doi:10.1016/j.jpowsour.2008.09.104

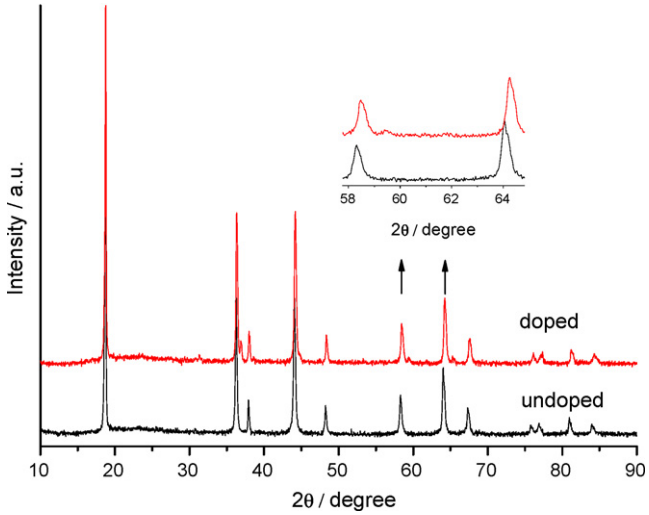

Fig. 1. XRD patterns of spinel samples.

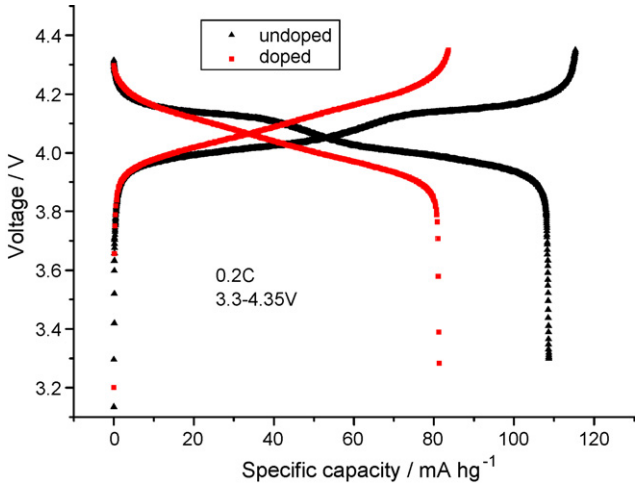

Fig. 2. Initial charge–discharge curves of samples.

5.3 mm × width 34.0 mm × height 50.0 mm. The full cell contain excess amount of electrolyte, about 3.2 g electrolyte was injected, the amount of electrolyte is enough to avoid influences on the cycle life.

Electrochemical test in the voltage region of 3.3–4.35 V (half cell) was performed with a constant charge/discharge rate of 0.2*C* (1*C* = 100 mA g^{-1} on undoped spinel, 80 mA g^{-1} on undoped spinel) at room temperature. The full cell was cycled in the voltage region of 3.2–4.2 V at charge/discharge rate of 2*C* at room temperature and at charge/discharge rate of 1*C* at 55 °C.

3. Results and discussion

XRD patterns of the spinels $LiMn_2O_4$ are shown in Fig. 1. All samples were identified as spinel structure, no impurity peaks could be observed, all diffraction peaks shift to higher 2θ angles. Table 1 gives the lattice parameter value of samples, the doped spinel has a smaller lattice parameter (8.2007 Å) value compared with the undoped spinel (8.2218 Å). It is confirmed that the incorporation of Co^{3+} (ionic radius 0.53 Å) into the spinel lattice should result in the decrease in quantity of the larger Mn^{3+} (ionic radius 0.66 Å) and shrinkage of unit cell volume [20], this could restrain the spinel structural change during cycling.

The initial charge–discharge capacity of samples are shown in Table 1 and Fig. 2. The initial charge–discharge capacity of undoped spinel was 115.3 mAh g^{-1} and 108.7 mAh g^{-1}, respectively, that decreased to 83.6 mAh g^{-1} and 81.3 mAh g^{-1} on the doped spinel, the initial charge–discharge efficiency greatly increased from 94.3% to 97.3%. In undoped spinel, the two charge–discharge plateaus in 4 V region are obvious. However, in doped spinel, the two charge–discharge plateaus in 4 V region are not so obvious. It could be ascribed to substitution of Mn by Co and Li reduced the capacity of spinel in 4 V region since these doped ions are inactive in this potential range.

Table 1
Initial charge–discharge capacity of samples.

Sample name	Initial charge capacity (mAh g^{-1})	Initial discharge capacity (mAh g^{-1})	Efficiency (%)
Undoped	115.3	108.7	94.3
Doped	83.6	81.3	97.3

In order to compare the cycling performance between undoped and doped spinel, we presented the comparison of cycling performance on both half cell and full cell (Figs. 3 and 4, respectively). The cycling performance of samples on half cells is shown in Fig. 3. When cycled at the current rate of 1*C*, the capacity retention was 96.6% after 30 cycles on undoped spinel, which was 98.4% on the doped spinel. Doped spinel showed better cycling performance than undoped spinel.

Fig. 4 shows cycling performance of graphite/spinel cells cycled at room temperature. At the 300th cycle, the capacity retention was 62% on undoped, which was 94% on doped spinel. Doped spinel exhibited superior capacity retention, which maintained up to 86% after 1000 cycles. According to the initial capacity and capacity retention value, after 183 cycles, doped spinel delivered higher specific capacity than undoped spinel. Capacity retention of the doped spinel was slightly higher than the undoped spinel on the half cell, which can reflect the short-term cycling performance, but there was distinct difference on the full cell after long-term cycling. A similar comparison of cycling performance between half cell and full cell can be found on Xia's report [18]. Although initial specific capacity was reduced, partial substitution of Mn with Co and Li can improve the cycling performance of spinel cathode.

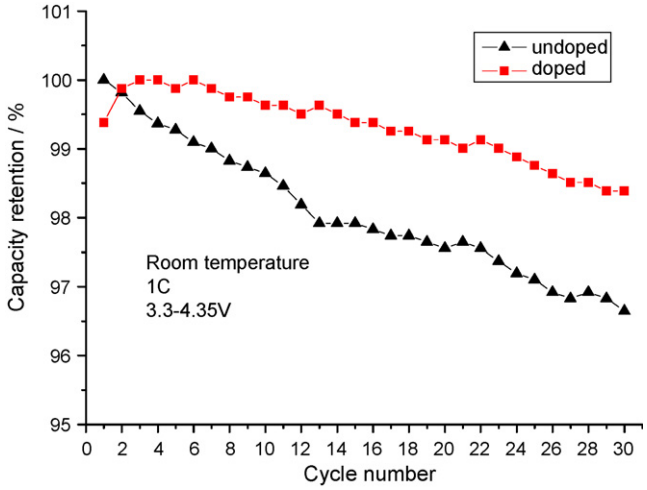

Fig. 3. Capacity retention of Li/spinel cells.

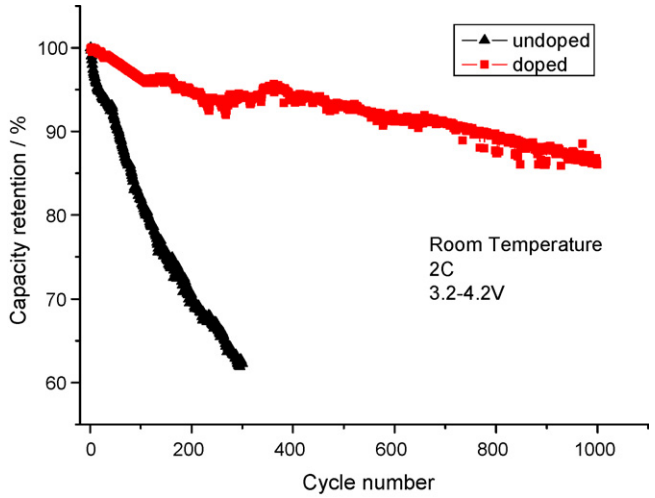

Fig. 4. Capacity retention of graphite/spinel cells.

Fig. 5 shows cycling performance of graphite/spinel cells cycled at 55 °C. At the 40th cycle, the capacity retention of undoped spinel was less than 45%. On the contrary, the capacity retention of the Co and Li doped spinel had maintained more than 92% at the 40th cycle, it was 85% at the 100th cycle. The doped spinel exhibits significant better cycling performance than undoped spinel when cycled at 55 °C. It is worth notice that the capacity retention curves at room temperature and 55 °C shows the same tendency, it can be explained that the capacity fading was accelerated when cycled at elevated temperature.

Fig. 6 shows the differential capacity profile of graphite/spinel cells cycled at 2*C* between 3.2 V and 4.2 V. Both cells have the same anode, just different on spinel cathode. However, the differential capacity profiles of cells are quite different. On undoped spinel cathode, an obvious peak deformation could be observed when cycled more than 100 cycles. The peaks during charge step shifted to higher voltage quickly. During the discharge step, the peaks shifted to lower voltage quickly. This can be explained by the impedance increase of the cell, which may caused by the loss of contact between active material and conductive agent, surface layer formation and reprecipitation of new phases. That is quite different on the doped spinel cathode, the peaks shifted to higher voltage during both charge and discharge steps. It can be explained that the

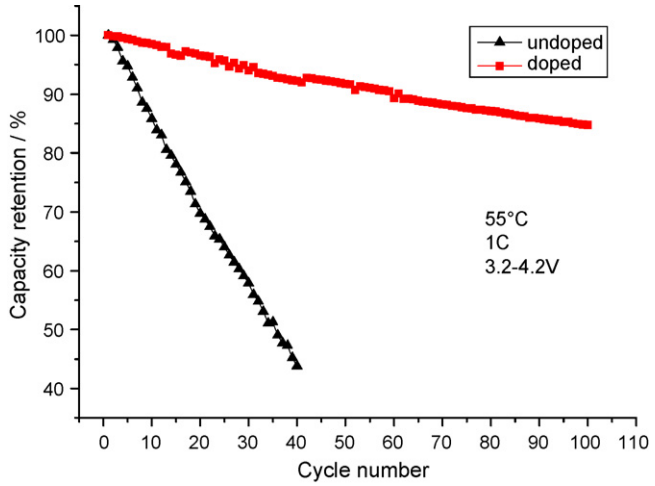

Fig. 5. Capacity retention of graphite/spinel cells cycled at 55 °C.

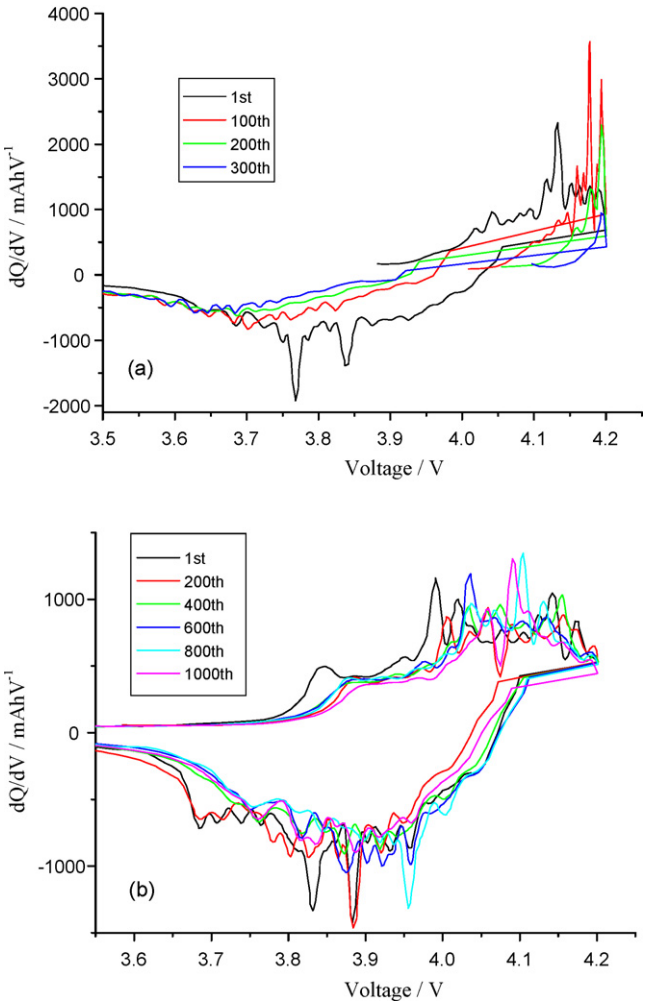

Fig. 6. Differential capacity profiles of graphite/spinel cells cycled at 2*C* between 3.2 V and 4.2 V: (a) undoped spinel cathode and (b) doped spinel cathode.

continuous loss of accessible lithium due to the formation of new solid electrolyte interphase (SEI) layers during cycling, which indirectly increases the potential of the positive electrode. This result is well consistent with Amine's research [21]. After 400 cycles, the profiles changed little. It appears that the differential capacity profiles on doped spinel cathode are more stable than undoped spinel cathode.

Table 2 shows the specific surface area and Mn dissolution value of samples. The specific surface area decreased from 1.044 $m^2\ g^{-1}$ to 0.765 $m^2\ g^{-1}$ as the Co and Li doped into spinel, while the Mn dissolution value by soaking samples in electrolyte solution at 55 °C for 7 days decreased from 1.33% to 0.78%. Mn dissolution assessment is a kind of simulation technique to compare the Mn dissolution between undoped and doped spinel. A similar Mn dissolution test had been conducted by Choi and Manthiram [5], which was range from 0.9% to 3.9% on doped cathode. Chemical dissolution of lithium manganese spinel in electrolyte is a crucial problem, especially at elevated temperatures. The Mn^{3+} ions disproportionated to Mn^{2+}

Table 2
Specific surface area and Mn dissolution of samples.

Sample name	Specific surface area ($m^2\ g^{-1}$)	Mn dissolution (%)
Undoped	1.044	1.33
Doped	0.765	0.78

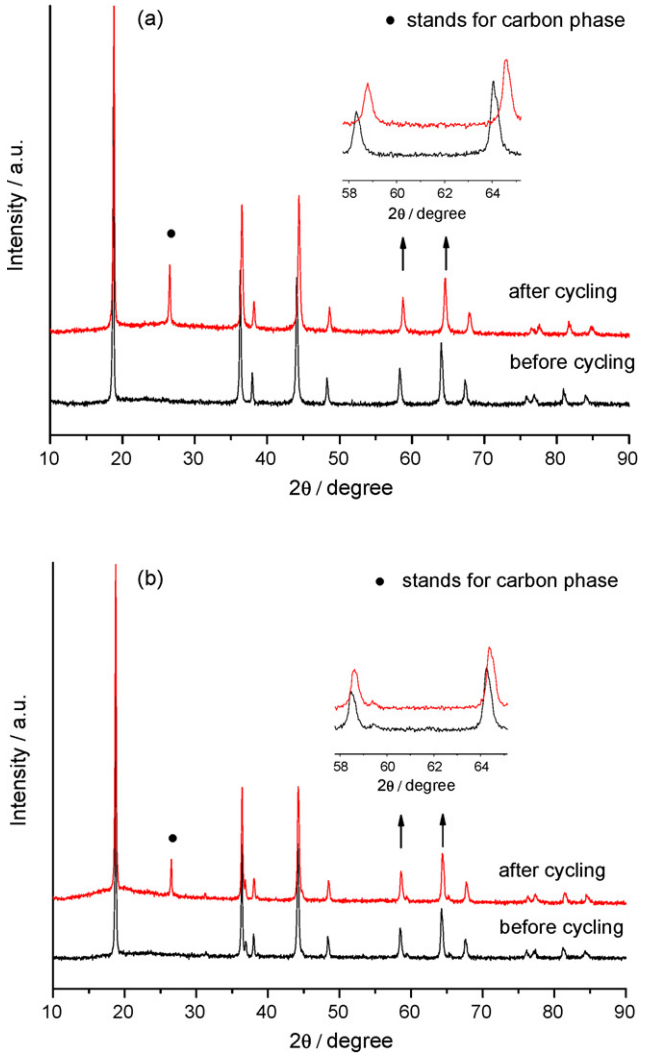

Fig. 7. XRD patterns of spinel cathodes in graphite/spinel cells after cycling: (a) undoped spinel cathode after 300 cycles and (b) doped spinel cathode after 1000 cycles.

ions and Mn^{4+} ions, the Mn^{2+} ions are soluble in the electrolyte. Mn dissolution leads to loss of active material, more seriously, the Mn^{2+} could be deposited on the graphite anode and then causes capacity loss of the graphite anodes during cycling or storage. These data show that Mn dissolution into electrolyte at 55 °C can be reduced by 41% on doped spinel, Mn dissolution can be effectively suppressed due to lower specific surface area by Co and Li doping.

Fig. 7 compares the XRD patterns of spinel cathodes at stage of discharge cycled at room temperature. The peaks of both electrodes shifted to higher 2θ angles after cycling. Table 3 gives the lattice parameter value of samples before and after cycling. Lattice parameter of undoped spinel cathode was 8.1648 Å, the lattice parameter difference Δa was 0.0570 Å after 1000 cycles. However, lattice parameter of doped spinel cathode was 8.1906 Å, the lattice parameter difference Δa was 0.0101 Å after 300 cycles. Compared with undoped spinel cathode, Δa of doped spinel cathode was reduced by 82%. The structural change is responsible for the capacity fading on cycling. The loss of crystallinity on cycling may hinder the three-dimensional diffusion of lithium ions in the spinel lattice and consequently lead to increased polarization and capacity fade arising from impedance growth, which can well interpret the differential capacity profile of graphite/undoped spinel cells have been discussed in Fig. 6(a). Cobalt and lithium doubly doped spinel cathode maintained good crystallinity and resulted in greatly enhanced cycling performance.

Table 3
Lattice parameters of samples: undoped spinel cathode after 300 cycles, doped spinel cathode after 1000 cycles.

Sample name	Before cycling (Å)	After cycling (Å)	Δa (Å)
Undoped	8.2218	8.1648	0.0570
Doped	8.2007	8.1906	0.0101

4. Conclusions

In this study, we have successfully prepared Co and Li doubly doped spinel $LiMn_2O_4$. Compared with undoped spinel, the Co and Li doubly doped spinel exhibits superior capacity retention. The capacity retention of graphite/doped spinel was more than 86% after 1000 cycles (2*C* rate) at room temperature, and maintained 85% after 100 cycles (1*C* rate) at 55 °C. The differential capacity profiles on doped spinel cathode are much more fixed than undoped spinel cathode. Mn dissolution into electrolyte at 55 °C was reduced by 41%, the lattice parameter difference Δa was reduced by 82% on doped spinel cathode after cycling. We conclude that the greatly enhanced cycling performance is attributed to slow down of manganese dissolution in spinel cathode and stabilize the spinel structure during cycling.

Acknowledgment

This work has been financially supported by the National High-tech R&D Program of China (863 Program) under Grant No. 2006AA11A160.

References

[1] T. Kakuda, Y. Uematsu, Journal of Power Sources 167 (2007) 499–503.
[2] Z. Bakenov, I. Taniguchi, Solid State Ionics 176 (2005) 1027–1034.
[3] J. Vetter, P. Novak, M.R. Wagner, C. Veitb, K.-C. Möller, J.O. Besenhard, M. Winter, M. Wohlfahrt-Mehrens, C. Vogler, A. Hammouche, Journal of Power Sources 147 (2005) 269–281.
[4] Z. Chen, K. Amine, Journal of the Electrochemical Society 153 (2) (2006) A316–A320.
[5] W. Choi, A. Manthiram, Journal of the Electrochemical Society 154 (7) (2007) A614–A618.
[6] J.H. Lee, J.K. Hong, D.H. Jang, Y.-K. Sun, S.M. Oh, Journal of Power Sources 89 (2000) 7–14.
[7] A. Paolone, R. Cantelli, B. Scrosati, P. Reale, M. Ferretti, C. Masquelier, Materials Science and Engineering A 442 (2006) 220–223.
[8] F.-Y. Shih, K.-Z. Fung, Journal of Alloys and Compounds 430 (2007) 320–329.
[9] Y.-P. Fu, C.-H. Lin, Y.-H. Su, S.-H. Wu, Journal of Power Sources 159 (2006) 215–218.
[10] S.B. Tang, M.O. Lai, L. Lu, Journal of Power Sources 164 (2007) 372–378.
[11] J. Tu, X.B. Zhao, G.S. Cao, D.G. Zhuang, T.J. Zhu, J.P. Tu, Electrochimica Acta 51 (2006) 6456–6462.
[12] A. Eftekhari, Solid State Communications 140 (2006) 391–394.
[13] L. Yu, X. Qiu, J. Xi, W. Zhu, L. Chen, Electrochimica Acta 51 (2006) 6406–6411.
[14] C.-H. Lu, S.K. Saha, Materials Science and Engineering B 79 (2001) 247–250.
[15] J.-M. Han, S.-T. Myung, Y.-K. Sun, Journal of the Electrochemical Society 153 (7) (2006) A1290–A1295.
[16] M. Sano, T. Hattori, T. Hibino, M. Fujita, Electrochemical and Solid-State Letters 10 (12) (2007) A270–A273.
[17] B. Deng, H. Nakamura, M. Yoshio, Journal of Power Sources 141 (2005) 116–121.
[18] Y. Xia, Q. Zhang, H. Wang, H. Nakamura, H. Noguchi, M. Yoshio, Electrochimica Acta 52 (2007) 4708–4714.
[19] M. Takahashi, T. Yoshida, A. Ichikawa, K. Kitoh, H. Katsukawa, Q. Zhang, M. Yoshio, Electrochimica Acta 51 (2006) 5508–5514.
[20] T. Yi, X. Hu, K. Gao, Journal of Power Sources 162 (2006) 636–643.
[21] Z. Chen, K. Amine, Journal of the Electrochemical Society 153 (7) (2006) A1279–A1283.